Production of high-order Bessel beams with a Mach–Zehnder interferometer

Carlos López-Mariscal, Julio C. Gutiérrez-Vega, and Sabino Chávez-Cerda

A new experimental setup is demonstrated to produce high-order Bessel beams. It is based on the field decomposition of the Bessel beam into its even and odd field components. The implementation is performed over the spectral components with a Mach–Zehnder interferometer that synthesizes the components into the desired Bessel beam. The main advantage of our setup is that the required annular transmittances have only discrete phase changes of π radians instead of a continuous change of phase.

OCIS codes: 350.5500, 050.1960, 140.3300.

1. Introduction

In past years, a number of practical ways to generate Bessel beams have been found. For example, use of passive optical systems fed by laser light with a ring aperture placed at the focal distance of a positive lens,[1,2] refractive or diffractive axicons,[3–5] holographic methods,[6,7] or diffractive phase elements[8] has been reported. In contrast to passive methods, several active schemes have been proposed to produce finite-aperture approximations of Bessel and Bessel–Gauss beams in resonators.[9–13]

Because of its simplicity, the experimental arrangement proposed originally by Durnin *et al.*[1,2] is one of the most used setups to generate nondiffracting beams in the laboratory; however, this technique has a disadvantage in the case of high-order Bessel beams (HOBBs): The complex transmittance $\exp(im\varphi)$ required by the ring aperture is not easily obtained.

In this paper we present a novel experimental arrangement to generate HOBBs. With our setup we use annular transmissive elements with discrete phase changes of π instead of the continuous phase change $m\varphi$ as required by the original setup proposed by Durnin. The new arrangement is based on the decomposition of the HOBB into its even and odd parts, and the reconstruction is made with a Mach–Zehnder interferometer. The arrangement we propose involves only simple optical components that are readily available in the laboratory. In this paper we extend previous research on the production of Bessel beams.

2. Durnin's Setup and Bessel Beams

We briefly describe Durnin's setup and Bessel beams to establish notation and to provide a reference point for necessary formulas. The representation in terms of plane waves of an arbitrary nondiffracting beam is written as[14]

$$U(x, y, z \geq 0) = \exp(ik_z z) \int_0^{2\pi} A(\varphi)\exp[ik_t(x \cos \varphi + y \sin \varphi)]\mathrm{d}\varphi, \quad (1)$$

where $A(\varphi)$ is the continuous or discrete complex angular spectrum, and $k_t = k \sin \theta_0$; $k_z = k \cos \theta_0$ are the transverse and longitudinal components of the wave vector $\mathbf{k}$. The integral in Eq. (1) represents a coherent superposition of plane waves whose wave vectors lie on the surface of a cone with semiangle $\theta_0 = \arccos(k_z/k)$ with respect to the z axis.

The angular spectrum $A(\varphi)$ defines the transverse structure of the field. Because the magnitude and phase of the function $A(\varphi)$ is arbitrary, an infinite number of nondiffracting wave fields with different transverse intensity shapes can be obtained. The case $A(\varphi) = \exp(im\varphi)$ has been extensively studied in the literature (see, for example, Refs. 1–4), and the

C. López-Mariscal and J. C. Gutiérrez-Vega (juliocesar@itesm.mx) are with the Photonics and Mathematical Optics Group, Tecnológico de Monterrey, Monterrey 64849, Mexico. S. Chávez-Cerda is with the Instituto Nacional de Astrofísica, Optica y Electrónica Apartado, Postal 51/216, Puebla 72000, Mexico.

Received 18 February 2004; revised manuscript received 27 April 2004; accepted 7 June 2004.

0003-6935/04/265060-04$15.00/0

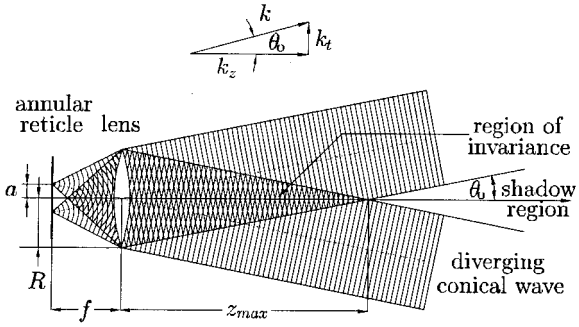

Fig. 1. Simple experimental setup used to generate nondiffracting beams.

generated field corresponds to the mth-order Bessel beam:

$$U(\rho, \phi, z) = J_m(k_t\rho)\exp(im\phi)\exp(ik_z z), \qquad (2)$$

which reduces to the fundamental J_0 Bessel beam when $m = 0$.

Durnin's setup is depicted in Fig. 1. A screen with an annular slit of radius a and transmittance $A(\varphi)$ is placed in the focal plane of a lens of radius R and focal length f. The ring is then illuminated by a monochromatic plane wave with wave number $k = w/c$ so that each point along the slit can be regarded as a point source of spherical waves that the lens transforms into plane waves. In this setup, the nondiffracting beam is generated beyond the lens within the conical region where the plane waves superpose. The conical semiangle θ_0 is written as $\theta_0 = \arctan(a/f)$. The geometric parameters of the arrangement define the components of the wave number to be

$$k_t = k \sin\theta_0 = ka(a^2 + f^2)^{-1/2}, \qquad (3)$$

$$k_z = k \cos\theta_0 = kf(a^2 + f^2)^{-1/2}. \qquad (4)$$

Because of the finite extent of the lens, the nondiffracting beam propagates a finite distance given by $z_{\max} = fR/a$ (see Fig. 1).

3. Splitting of a High-Order Bessel Beam

The key of the experimental setup we propose to generate HOBBs is the splitting of the Bessel beam [Eq. (2)] into an even field U_1 (Bessel cosine beam) and an odd field U_2 (Bessel sine beam) as follows:

$$\begin{aligned} U &= U_1 + iU_2 \\ &= J_m(k_t\rho)\cos(m\phi)\exp(ik_z z) \\ &\quad + iJ_m(k_t\rho)\sin(m\phi)\exp(ik_z z). \end{aligned} \qquad (5)$$

Both fields U_1 and U_2 are independent solutions of the Helmholtz equation in circular cylindrical coordinates, and consequently they are nondiffracting beams. The complex number i can be expressed as $\exp(i\pi/2)$ showing that there is an overall phase difference of one of the interfering fields with respect to the other.

In Fig. 2 we show the transverse amplitude and phase distributions of the constituent fields U_1 and U_2 for a first-order Bessel beam. Note that the transverse phase distributions of the Bessel cosine and Bessel sine beams exhibit sudden changes of π radians, in particular white regions represent a value of zero and black regions represent a value of π. On the other hand, the phase distribution of the HOBB is continuous and increases angularly according to $m\phi$.

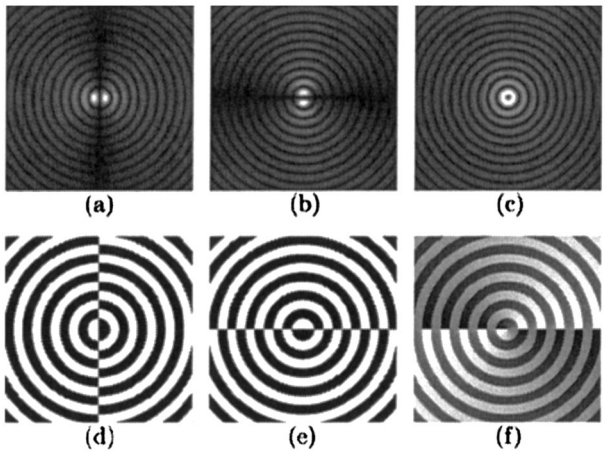

Fig. 2. Amplitude and phase distributions of the first-order (a) and (d) Bessel cosine, (b) and (e) Bessel sine, and (c) and (f) Bessel beams. In the phase distributions, white regions represent a value of zero and black regions represent a value of π.

Because the Bessel cosine and Bessel sine beams are nondiffracting beams themselves, they can be produced separately by use of Durnin's setup described in Section 2. The required transmittances are

$$\mathbb{T}_1(\varphi) = \cos(m\varphi), \qquad \mathbb{T}_2(\varphi) = \sin(m\varphi), \qquad (6)$$

respectively. In principle, we can construct a HOBB by interfering the fields U_1 and U_2 if the appropriate phase delay of $\pi/2$ between them is introduced.

4. Experiment and Results

To generate the HOBBs we interfere the Bessel cosine and Bessel sine beams with the same transverse constant k_t using the proposed Mach–Zehnder setup depicted in Fig. 3. Each constituent field is independently produced by the setup described in Section 2. Both fields are linearly polarized, and their electric vectors are parallel to each other. A phase-shifting glass plate is inserted in path 2 to adjust the relative phase difference between the arms. The mth-order Bessel beam is obtained once both fields are set to interfere by means of the second beam splitter.

We first describe the generation of the Bessel cosine and Bessel sine beams. In reference to Fig. 1, we spatially filter the light from a linearly polarized 15-mW He–Ne laser at 632.8 nm by focusing it with a 10× objective into a 25-μm pinhole. By using a well-corrected lens, we formed a collimated beam that passed through an annular slit that is 45 ± 7 μm thick and has a 0.750-mm radius. The transmit-

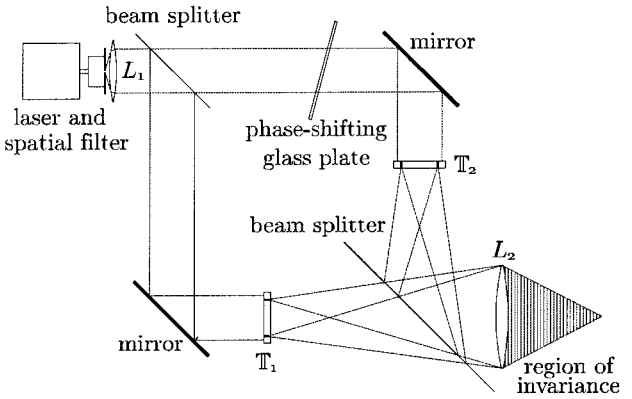

Fig. 3. Mach–Zehnder setup to produce HOBBs. Transmittances T_1 and T_2 are placed at a focal distance from the lens.

tance of the ring was modulated in amplitude and phase by the functions in Eqs. (6) for each of the arms, respectively. Behind the slit there was a second (well-corrected) lens with a 15-cm focal length. With this setup, the transverse wave number is computed to be $k_t = 5.0 \times 10^4\ \mathrm{m}^{-1}$.

We fabricated the annular transmittances by superimposing three layers: an annular slit of radius a, a photographic film accounting for the amplitude of the cosine (or sine) function $|\cos(m\varphi)|$, and a glass plate accounting for the sign of the cosine (or sine) function $\exp[i\Phi(\varphi)]$, where $\Phi(\varphi)$ is zero when the cosine is positive and π when it is negative.

As the amplitude $|\cos(m\varphi)|$ takes on only real and positive values, it can be easily generated by means of pure amplitude transparencies. In our case, the amplitude distribution was calculated with the aid of a computer program that maps the desired values of amplitude as a function of the angular coordinate using gray-scale values. This map is then displayed in a flat 16-in. (41-cm) LCD monitor and then photoreduced onto a 35-mm photographic film. We measured the overall irradiance levels to be within the linear range of the photographic film and made several photoreductions at different exposure times to ensure accuracy in the process and the desired results.

On the other hand, the π changes of phase required by $\exp[i\Phi(\varphi)]$ are achieved by means of thin glass slides properly placed on a uniform transparent plate. The plate with the glass slides is superimposed to the amplitude film and the annular slit, resulting in a layered diffractive optical element with the desired annular transmittance with angular variation. We stress that these transmittances exhibit phase changes of π radians that are easier to fabricate in the laboratory than the continuous phase transmittances $\exp(im\varphi)$.

The transverse patterns of the first-order Bessel cosine and Bessel sine beams at the plane of the output lens are shown in Fig. 4. They were observed at different distances and were practically identical within the expected propagation range. We note a good agreement with the theoretical expressions

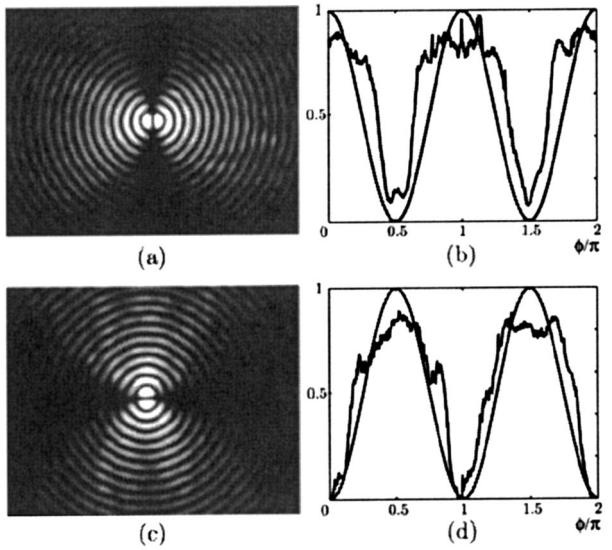

Fig. 4. (a) and (c) Photographic images of the first-order Bessel cosine and Bessel sine beams and (b) and (d) intensity variation with angular position for the fourth lobes.

$J_1^2(k_t\rho)\cos^2\phi$ and $J_1^2(k_t\rho)\sin^2\phi$ depicted in Fig. 2. The variation of the intensity as a function of the normalized angle φ/π for the fourth lobes is shown in Figs. 4(b) and 4(d). The deviations of the patterns with respect to the theoretical predictions are produced by the finite thickness of the annular slit.

Once the Bessel cosine and Bessel sine beams are generated, they are interfered with the Mach–Zehnder setup shown in Fig. 3. We kept the same k_t for both constituent beams by using two identical ring slits with the same diameter. The length of the paths between the splitters was approximately 30 cm. As required by Eq. (5), the HOBB is observed when the relative phase difference between the fields U_1 and U_2 is $\pi/2$. Because the path difference between the arms introduces an arbitrary phase difference, a compensating glass plate is inserted in path 2, and its inclination is carefully adjusted so that the two optical paths differ by $\pi/2$ rad.

Figure 5 shows the observed intensity distribution of the first-order Bessel beam produced with the Mach–Zehnder setup. The corresponding theoretical prediction is shown in Fig. 2(c). The patterns were measured with a charge-coupled device (CCD) and by a computer frame grabbing card and software at the planes $z = 1, 2, \ldots, 6$ m behind the output beam splitter. Measurements indicate that the separation between consecutive rings is approximately 65 μm, in agreement with the predicted value $\pi/k_t \simeq 63.3$ μm. By comparing the images, we note that the lobes of the beam retain their sizes as the beam propagates. Note the effect of the conical region of invariance on the transverse extent of the Bessel beam. The geometric model predicts a maximum propagation distance of up to 7.5 m. There are several potential sources for the slightly uneven appearance of the Bessel beam profile, such as film

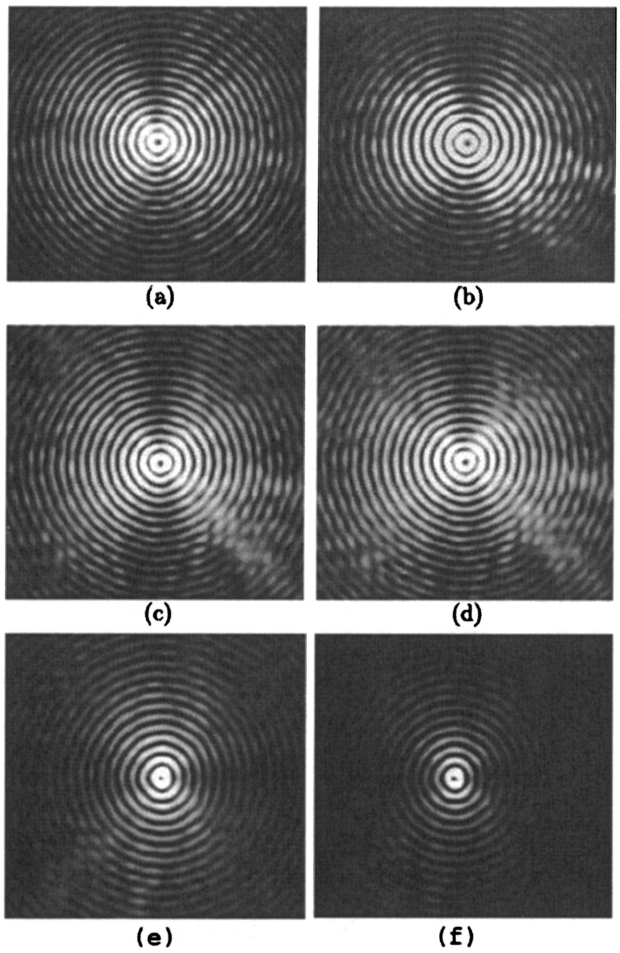

Fig. 5. Photographic sequence of the first-order Bessel beam at planes $z = 1, 2, 3, 4, 5$, and 6 m. Image size is 1.8 mm $\times$ 1.8 mm.

amplitude variations and inhomogeneities, residual aberrations in the optical system, astigmatism introduced by a slight misalignment of the interferometer, or a combination of these factors.

5. Conclusions

We have introduced a novel method for generating HOBBs using an experimental setup based on a Mach–Zehnder interferometer. The decomposition of the Bessel beam into its constituent even and odd spatial components allows us to deal with annular real transmittances involving discrete changes of the phase of π radians instead of transmittances with continuous phase changes. This Mach–Zehnder setup can be used to produce other types of nondiffracting beams with similar parity properties, for example, high-order Mathieu beams.[15,16]

This research was partially supported by Consejo Nacional de Ciencia y Tecnología in México and by the Tecnológico de Monterrey Research Chair in Optics grant CAT-007.

References

1. J. Durnin, "Exact solutions for nondiffracting beams. I. The scalar theory," J. Opt. Soc. Am. A **4,** 651–654 (1987).
2. J. Durnin, J. J. Micely, Jr., and J. H. Eberly, "Diffraction-free beams," Phys. Rev. Lett. **58,** 1499–1501 (1987).
3. G. Indebetouw, "Nondiffracting optical fields: some remarks on their analysis and synthesis," J. Opt. Soc. Am. A **6,** 150–152 (1989).
4. G. Scott and N. McArdle, "Efficient generation of nearly diffraction-free beams using an axicon," Opt. Eng. **31,** 2640–2643 (1992).
5. J. H. McLeod, "The axicon: a new type of optical element," J. Opt. Soc. Am. **44,** 592–597 (1954).
6. J. Turunen, A. Vasara, and A. T. Friberg, "Holographic generation of diffraction-free beams," Appl. Opt. **27,** 3959–3962 (1988).
7. A. Vasara, J. Turunen, and A. T. Friberg, "Realization of general nondiffracting beams with computer-generated holograms," J. Opt. Soc. Am. A **6,** 1748–1754 (1989).
8. W.-X. Cong, N.-X. Chen, and B.-Y. Gu, "Generation of nondiffracting beams by diffractive phase elements," J. Opt. Soc. Am. A **15,** 2362–2364 (1998).
9. K. Uehara and H. Kikuchi, "Generation of nearly diffraction-free laser beams," Appl. Phys. B **48,** 125–129 (1989).
10. P. Pääkkönen and J. Turunen, "Resonators with Bessel-Gauss modes," Opt. Commun. **156,** 359–366 (1998).
11. J. Rogel-Salazar, G. H. C. New, and S. Chávez-Cerda, "Bessel-Gauss beam optical resonator," Opt. Commun. **190,** 117–122 (2001).
12. A. N. Khilo, E. G. Katranji, and A. A. Ryzhevich, "Axicon-based Bessel resonator: analytical description and experiment," J. Opt. Soc. Am. A **18,** 1986–1992 (2001).
13. J. C. Gutiérrez-Vega, R. Rodriguez-Masegosa, and S. Chávez-Cerda, "Bessel–Gauss resonator with spherical output mirror: geometrical- and wave-optics analysis," J. Opt. Soc. Am. A **20,** 2113–2122 (2003).
14. G. N. Watson, *A Treatise on the Theory of Bessel Functions* (Cambridge U. Press, Cambridge, UK, 1987), pp. 651–654.
15. J. C. Gutiérrez-Vega, M. D. Iturbe-Castillo, and S. Chávez-Cerda, "Alternative formulation for invariant optical fields: Mathieu beams," Opt. Lett. **25,** 1493–1495 (2000).
16. J. C. Gutiérrez-Vega, M. D. Iturbe-Castillo, G. A. Ramírez, E. Tepichín, R. M. Rodríguez-Dagnino, S. Chávez-Cerda, and G. H. C. New, "Experimental demonstration of optical Mathieu beams," Opt. Commun. **195,** 35–40 (2001).